Article citation info:
Szymański GM, Wyrwas B, Klekowicki M, Strugarek K, Nowak M, Ludwiczak A et al. Simulation research of the feasibility of developing a multi-fuel valved pulsejet engine. Combustion Engines. 0000;XXX(X):xx-xx. https://doi.org/10.19206/CE-203139

Grzegorz M. SZYMAŃSKI
Bogdan WYRWAS
Mikołaj KLEKOWICKI
Klaudia STRUGAREK
Malwina NOWAK
Aleksander LUDWICZAK
Alicja SZYMAŃSKA

Combustion Engines
Polish Scientific Society of Combustion Engines

Simulation research of the feasibility of developing a multi-fuel valved pulsejet engine

ARTICLE INFO

Received: 13 February 2025
Revised: 19 March 2025
Accepted: 20 March 2025
Available online: 10 April 2025

The article provides an overview of the design and operation of pulse jet engines alongside a historical perspective on their development. It examines a selection of readily available fuels with diverse physicochemical properties, including methane, methanol, ethanol, gasoline, and LPG. A detailed chemical and energetic analysis of the combustion process for each fuel is conducted to determine key kinematic and thermodynamic parameters critical for the design and optimization of pulse jet engines. Computational methods and numerical tools used for simulating combustion chamber processes are discussed, with a focus on numerical analyses performed in the ANSYS environment. These simulations evaluate the impact of geometric parameters on the specific engine work, enabling the identification of optimal design solutions and key areas requiring further research and modifications. The study concludes by exploring potential design changes necessary for adapting pulse jet engines to operate efficiently with multiple fuel types. This includes considerations related to material selection for resistance to high temperatures and aggressive combustion conditions, as well as solutions for effective fuel distribution.

Key words: *pulsejet engines, alternative fuels, numerical analysis, CFD, design optimization*

This is an open access article under the CC BY license (http://creativecommons.org/licenses/by/4.0/)

1. Introduction

The contemporary battlefield is characterized by high dynamics and variability in operational conditions, which places critical importance on both the responsiveness and adaptive capabilities of armed forces. Consequently, the development of innovative propulsion solutions, including pulse jet engines, addresses the growing demand for efficient, reliable, and easily adaptable propulsion systems capable of operating in demanding environments. A particularly significant aspect of these efforts is the ability to utilize a variety of fuels, driven by both logistical considerations and the need to ensure operational continuity under diverse tactical conditions.

Since the early development of jet propulsion, engineers and researchers have consistently aimed to enhance the operational parameters of propulsion systems, such as reducing their weight and expanding the range of usable fuels. Experiences derived from contemporary military operations indicate that flexibility in energy source selection can be a critical factor in determining the effectiveness of combat missions. This is especially relevant in regions with limited logistical infrastructure, where the ability to utilize locally available fuels or unconventional fuel blends becomes increasingly significant. At the same time, pulse jet engines, due to their relatively simple design and high energy density, exhibit considerable potential for military applications.

The growing interest in the concept of a multi-fuel pulse jet engine stems not only from the strategic and operational requirements of the modern battlefield but also from the rapid advancement of technologies in materials science, automation, and advanced control systems. Progress in these areas enables the design and construction of pulse systems characterized by increased thermal and mechanical resistance while facilitating integration with unmanned combat platforms and cruise missiles.

2. Objectives and scope of the work

The main goal of this article is to initiate systematic research on the construction and application of a multi-fuel pulsejet engine, leading to a better understanding of the combustion mechanisms and flow dynamics in this type of propulsion system. In particular, the work aims to deepen both theoretical and practical knowledge regarding the selection of different fuels and their impact on efficiency, combustion stability, and engine durability. This is of significant importance for both further scientific and experimental applications, as well as technological implementations. The results and conclusions obtained will be used to develop design guidelines, which may contribute to the creation of a prototype system powered by various types of fuel in the future. The authors aim to lay the foundation for further work, addressing not only design and material aspects but also safety issues and the potential integration of a multi-fuel pulsejet engine with unmanned aerial platforms.

3. Literature review

Research on pulse jet engines has a long history, dating back to the first half of the 20th century. The earliest designs – most notably the German Argus As 014 engine used in V-1 missiles during World War II – sparked widespread interest in the principle of pulse combustion. Although initially employed solely in simple military systems, significant advancements over the years in understanding flow and combustion mechanisms have enabled the development of new variations and applications of pulse jet engines [20].

The scientific literature contains numerous publications focusing on the theoretical and experimental analysis of pulse jet engines. Complementing these studies are works dedicated to improving the fuel-air mixture, which emphasize the development of optimal fueling conditions to ensure combustion stability across a wide range of temperatures and pressures [22, 26].

A particularly important aspect, addressed in the context of this study, is the ability to power pulse jet engines with a variety of fuels. Research on the use of alternative fuels, including methanol, ethanol, and LPG, has been conducted with the aim of improving supply logistics and reducing environmental impact. The 1990s and early 21st century saw a growing interest in low-emission fuels [12, 13] and high-energy-density fuels, focusing on the evaluation of combustion characteristics and pollutant emissions for various fuels in pulse jet engines and related designs, such as detonation engines [23].

Advancements in simulation tools, such as ANSYS Fluent and CFX, have significantly expanded the capabilities for modeling phenomena associated with the operation of pulse jet engines. Numerical analyses enable precise replication of the pulse combustion process and the simulation of various geometric configurations without the need to build prototypes for every considered modification. The literature provides numerous examples of the application of these tools, including studies on optimizing combustion chamber shapes, controlling inlet flow swirl, and selecting the optimal fuel injection parameters. An example of a comprehensive numerical and experimental analysis of multi-fuel pulse jet engines is the work of Badanov et al., which presents a methodology for modeling fuel stream behavior and pressure wave dynamics [15, 17].

From a military application perspective, the development of pulse jet engines, including multi-fuel concepts, has garnered increasing interest due to their relatively simple design, low production and maintenance costs, and favorable thrust-to-weight ratio. These features enable their implementation in unmanned aerial platforms and short-range missiles. However, studies presented in the literature highlight the necessity of addressing numerous technical and material challenges, such as ensuring operation under extreme thermal conditions and maintaining structural integrity in cyclically fluctuating pressure fields [5].

4. Basic information about pulsejet engines

4.1. Structure of a pulsejet engine

The pulse jet engine is a type of combustion flow engine with a principle in which the combustion process occurs in a sequence of rapidly successive impulses. The operating cycle frequency of the engine is inversely proportional to its dimensions. For instance, small-scale model engines typically operate at frequencies of around 200–250 Hz, while the engine used in the German V-1 flying bomb reached approximately 45 Hz. The design of a pulse jet engine is exceptionally simple and lightweight compared to other jet engines with continuous exhaust flow, resulting in a favorable thrust-to-weight ratio. However, one of its major drawbacks is the high noise level (approximately 145 dB), which in practice limits its civilian applications and makes it more commonly used in the military sector. The basic components of a pulse jet engine include an air intake, combustion chamber, fuel injector, and nozzle (Fig. 1) [4, 11].

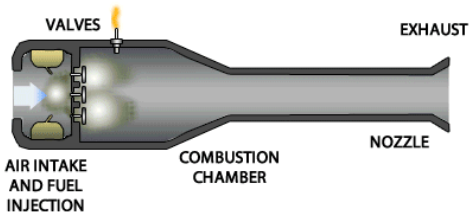

Fig. 1. Valved pulsejet engine cross-section [24]

4.2. Operation principles

In the initial phase of the operating cycle (Fig. 2a), air flowing through the intake mixes with fuel delivered directly into the combustion chamber. Subsequently (Fig. 2b), the mixture ignites, typically triggered by a spark. As a result of the rapid pressure increase in the combustion chamber, the intake valve closes [8].

In the next phase (Fig. 2c), the exhaust gases are expelled through the outlet channel, and their inertia causes a temporary drop in pressure within the combustion chamber below the ambient pressure. This allows the intake valve to reopen, and the receding flame initiates the next combustion phase. This entire process repeats multiple times in rapid succession, enabling the generation of continuous thrust.

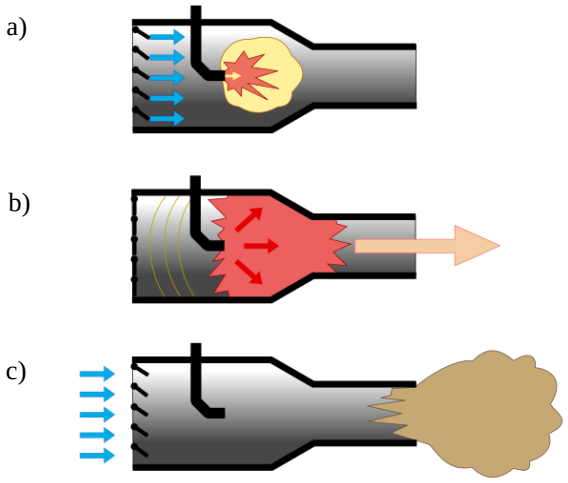

Fig. 2. Valved pulsejet engine working principles [25]

4.3. Ways to control pulsejet engine

Due to their design, pulse jet engines are divided into two primary categories: valved and valveless. In valved engines, the critical component is the intake valve, which can be controlled either mechanically (through the combustion cycle) or electronically. A drawback of mechanically actuated valves is their susceptibility to damage caused by high operational loads, as well as the occurrence of "backflow" at low flow rates, resulting from the limited speed of valve opening and closing. However, the mechanical valve can be designed as a membrane that allows airflow exclusively toward the combustion chamber, partially addressing the backflow issue [7, 8].

In valveless pulse jet engines, all moving parts are eliminated. Gas flow is controlled solely by the carefully designed geometry of the combustion chamber and the intake and exhaust channels. During combustion, the combustion products are expelled primarily through the exhaust channel, which has a larger cross-section, but some of the gases also flow backward through the intake. After the exhaust gases exit, the pressure in the combustion chamber drops below atmospheric pressure, allowing fresh air to enter and enabling the next ignition cycle.

Although, in a valveless design, a portion of the thrust appears to "escape" through the air intake, this does not result in a loss of useful thrust in practice. By curving the engine into a "U" shape (Fig. 3), both gas streams (exhaust and "backflow") can be directed in the desired direction, achieving a very favorable thrust-to-weight ratio [21].

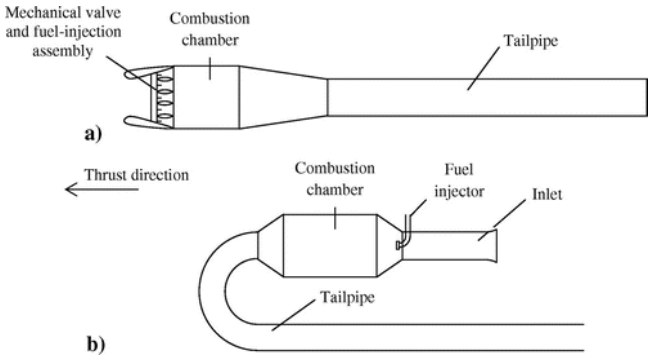

Fig. 3. Valved pulsejet engine a) and valveless pulsejet engine b) [7]

5. Physiochemical processes in pulsejet engine

5.1. Combustion in pulsejet engines

Combustion, from a chemical perspective, is a rapid and highly exothermic reaction between fuel and oxygen. Fuel refers to technical materials that release a significant amount of energy per unit of mass during the combustion process. The combustion reactions of individual fuels [3, 14, 17]:

Methane

$$CH_4 + 2O_2 \rightarrow CO_2 + 2H_2O \quad (1)$$

Methanol

$$2CH_3OH + 3O_2 \rightarrow 2CO_2 + 4H_2O \quad (2)$$

Ethanol

$$C_2H_5OH + 3O_2 \rightarrow 2CO_2 + 3H_2O \quad (3)$$

Gas

$$2C_8H_{18} + 25O_2 \rightarrow 16CO_2 + 18H_2O \quad (4)$$

LPG
Propane combustion:

$$C_3H_8 + 5O_2 \rightarrow 3CO_2 + 4H_2O \quad (5)$$

Butane

$$2C_4H_{10} + 13O_2 \rightarrow 8CO_2 + 10H_2O \quad (6)$$

Olefin's general reaction:

$$C_nH_{2n} + \frac{3n}{2}O_2 \rightarrow nCO_2 + nH_2O \quad (7)$$

The determination of the amount of energy released during combustion is governed by Hess's Law. The quantity of heat released or absorbed by a system depends on the initial and final states of the reaction rather than the specific pathway of the process. In the context of fuel combustion, this means that the enthalpy of the combustion reaction can be calculated [1].

Hess's Law can be expressed by the following equation:

$$\Delta H^\circ = \sum_i n_i \Delta H^\circ_{i\,p} - \sum_j n_j \Delta H^\circ_{j\,s} \quad (8)$$

where: ΔH° – enthalpy of reaction [kJ], i – number of product, j – number of subtract, n_i – number of moles of product number i, n_j – number of moles of subtract number j, $\sum n_i \Delta H^\circ_{i\,p}$ – the sum of changes in standard enthalpy of the products [kJ], $\sum n_j \Delta H^\circ_{j\,s}$ – the sum of changes in standard enthalpy of the subtracts [kJ].

The enthalpy of combustion is the difference between the enthalpy of the combustion products and the enthalpy of the reactants at a given temperature and pressure [9, 18]; it represents the amount of energy released as heat during the complete combustion of fuel. This value is expressed in units of kJ. Table 1 presents literature data on the enthalpy of combustion for the fuels considered in this study.

Table 1. Values of enthalpy of combustion for specific fuels [1]

Fuel	Enthalpy of combustion [kJ]
Methane	802
Methanol	726
Ethanol	1368
Gas	5470
LPG	2040

The enthalpy of combustion for individual fuels was calculated using equation (8). The enthalpy of combustion was determined for 1 mole of fuel in accordance with the stoichiometry of the given reaction. This approach aligns with the definition and practical application of enthalpy.

Table 2. Value of standardized enthalpy [1]

$\Delta H^\circ \left[\frac{kJ}{mol}\right]$							
Methane	Methanol	Ethanol	Gas	Propane	Butane	Carbon dioxide	Water
−74.8	−205.1	−234.2	−224.1	−104.7	−134.2	−393.52	−241.83

Methane

$$CH_4 + 2O_2 \rightarrow CO_2 + 2H_2O \quad (9)$$

$$\Delta H^\circ = \left(-393.52 + 2 \cdot (-241.83)\right) - (-74.8) \quad (10)$$

$$\Delta H^\circ = -802.38\ \text{kJ}$$

Methanol

$$CH_3OH + \frac{3}{2}O_2 \rightarrow CO_2 + 2H_2O \quad (11)$$

$$\Delta H^\circ = \left(-393.52 + 2 \cdot (-241.83)\right) - (-205.1) \quad (12)$$

$$\Delta H^\circ = -671.58\ \text{kJ}$$

Ethanol

$$C_2H_5OH + 3O_2 \rightarrow 2CO_2 + 3H_2O \quad (13)$$

$$\Delta H° = \left(2 \cdot (-393.52) + 3 \cdot (-241.83)\right) - (-234.2) \quad (14)$$

$$\Delta H° = -1278.33 \text{ kJ}$$

Gas

$$C_8H_{18} + \frac{25}{2}O_2 \rightarrow 8CO_2 + 9H_2O \quad (15)$$

$$\Delta H° = \left(8 \cdot (-393.52) + 9 \cdot (-241.83)\right) - (-224.1) \quad (16)$$

$$\Delta H° = -5100.53 \text{ kJ}$$

LPG

LPG is a mixture of propane and butane gases; therefore, the enthalpy of combustion was first calculated separately for each component. Subsequently, the value for the mixture was estimated based on its percentage composition. Propane combustion:

$$C_3H_8 + 5O_2 \rightarrow 3CO_2 + 4H_2O \quad (17)$$

$$\Delta H° = \left(3 \cdot (-393.52) + 4 \cdot (-241.83)\right) - (-104.7) \quad (19)$$

$$\Delta H° = -2043.18 \text{ kJ}$$

Butane combustion:

$$C_4H_{10} + \frac{13}{2}O_2 \rightarrow 4CO_2 + 5H_2O \quad (20)$$

$$\Delta H° = \left(4 \cdot (-393.52) + 5 \cdot (-241.83)\right) - (-134.2) \quad (21)$$

$$\Delta H° = -2649.03 \text{ kJ}$$

Enthalpy of combustion of LPG:

The propane and butane mixture is used in various proportions. For the purpose of the calculations, it was assumed that the gases constitute equal parts, with each making up 50% of the mixture.

$$\Delta H°_{LPG} = 0.5 \cdot (-2043.18) + 0.5 \cdot (-2649.03)$$

$$\Delta H° = -2346.105 \text{ kJ}$$

Table 3. Results of calculated combustion's enthalpy

Fuel	Calculated enthalpy [kJ/mol]
Methane	− 802.38
Methanol	− 671.58
Ethanol	− 1278.33
Gas	− 5100.53
LPG	−2346.11

The results of the calculated enthalpy of combustion are presented in Table 3, while literature values are provided in Table 1. These values are not equal. The discrepancies are likely due to different conditions under which the enthalpy determination processes were conducted. The enthalpy of combustion depends on the physical state of the reaction products, and thus the differences may arise from the consideration of different physical states of substances in various sources [1, 9, 16].

It is important not to confuse the enthalpy of combustion with the heat of combustion. While these are related concepts describing the energy released during combustion, they differ in meaning. Enthalpy is a thermodynamic quantity that defines the change in enthalpy during the combustion of 1 mole of a substance, representing the amount of energy obtainable from fuel decomposition while accounting for the differences in bond energies. In contrast, the heat of combustion refers to the total energy released during the combustion of a unit mass or volume of fuel. Enthalpy of combustion is a theoretical value associated with the thermodynamic analysis of the reaction, while the heat of combustion reflects practical conditions of energy release and the states of combustion products.

During fuel combustion, the amount of energy generated is denoted as H. Combustion of a given fuel is characterized by a maximum energy value, H_{mx}; however, in reality, this value is lower and depends on the oxidizer excess coefficient α. In engineering applications, air is the most commonly used oxidizer because it is widely available and cost-free. The energy value can be determined as follows:

$$H_{mx} = \frac{W_t}{1+L_t} \quad (22)$$

where: H_{mx} – maximum energy during combustion $\left[\frac{kJ}{kg}\right]$, W_t – combustion heat $\left[\frac{kJ}{kg}\right]$, L_t – theoretical air requirement $\left[\frac{\text{kg of air}}{\text{kg of fuel}}\right]$.

The heat of combustion of a fuel is the thermal energy released during the complete combustion of the fuel, which measures the energy content of the fuel. Table 4 presents the heat of combustion and the theoretical air demand for the specified fuels [19].

Table 4. Values of combustion heat and theoretical air demand for energy calculations [1]

Fuel	$W_t \left[\frac{kJ}{kg}\right]$	$L_t \left[\frac{\text{kg of air}}{\text{kg of fuel}}\right]$
Methane	50 000	17.2
Methanol	19 900	6.45
Ethanol	26 800	9.0
Gas	44 500	14.7
LPG	48 000	15.5

Methane

$$H_{mx} = \frac{50\,000}{1+17.2} \quad (23)$$

$$H_{mx} = 2747.25 \frac{kJ}{kg}$$

Methanol

$$H_{mx} = \frac{19\,900}{1+6.45} \quad (23)$$

$$H_{mx} = 2671.14 \frac{kJ}{kg}$$

Ethanol

$$H_{mx} = \frac{26\,800}{1+9} \quad (24)$$

$$H_{mx} = 2680 \frac{kJ}{kg}$$

Gas

$$H_{mx} = \frac{44\,500}{1+14.7} \quad (25)$$

$$H_{mx} = 2834.39 \frac{kJ}{kg}$$

LPG

$$H_{mx} = \frac{48\,000}{1+15.5} \quad (26)$$

$$H_{mx} = 2909.09 \frac{kJ}{kg}$$

Table 5. Calculation results of the maximum energy value during combustion

Fuel	Calculated maximum value of energy $\left[\frac{kJ}{kg}\right]$
Methane	2747.25
Methanol	2671.14
Ethanol	2680.00
Gas	2834.39
LPG	2909.09

Using spark plugs, combustion is initiated by a spark discharge, which acts as an internal energy source. A necessary condition for the combustion process to occur is the proper preparation of the combustible mixture. This preparation involves fuel atomization, evaporation, and mixing of fuel vapors with air. The intensity of fuel evaporation, which is crucial, can be enhanced by preheating the mixture. After the initial ignition by the spark, subsequent layers of fuel ignite as they come into contact with the hot combustion gases produced from the burning of the previous layer during laminar flow. The factors initiating ignition in the successive layers of the mixture include heat conduction from the combustion gases and the diffusion of active particles, such as free atoms or radicals, generated during the combustion of previous layers.

It has not yet been determined which of these phenomena controls the process. Therefore, there are two groups of theories explaining the laminar combustion of homogeneous mixtures: the group of diffusion theories and the group of thermal theories. Below, one of the simplest thermal theories is described [26, 27]:

$$q = c_p \rho u_L (T_Z - T_0) \quad (27)$$

where: q – heat flux $[\frac{kJ}{m^2 s}]$, c_p – specific heat $[\frac{kJ}{kgK}]$, ρ – density $[\frac{kg}{m^3}]$, u_L – speed of combustion $[\frac{m}{s}]$, T_0 – ambient temperature [K], T_Z – combustion temperature [K].

Table 6. Physical and thermodynamic parameters of fuels for energy calculations [1]

Compound	Methane	Methanol	Ethanol	Gas	LPG
$c_p \left[\frac{kJ}{kgK}\right]$	2.22	2.51	2.44	2.1	2.58
$\rho \left[\frac{kg}{m^3}\right]$	0.717	792	789	755	2.2
$u_L \left[\frac{m}{s}\right]$	0.41	0.25	0.32	0.4	0.36
T_0 [K]	293.15				
T_Z [K]	2223.15	2143.15	2193.15	2743.15	2253.15

Calculations of the amount of energy released during the combustion of methane were performed as follows:

$$q = 2.22 \cdot 0.717 \cdot 0.41 \cdot (2223.15 - 293.15) \quad (28)$$

$$q = 1259.54 \frac{kJ}{m^2 s}$$

Analogous calculations were performed for each fuel, and the results are presented in the table below.

Table 7. Calculation results of the amount of energy produced during combustion

Fuel	Calculated energy flux $\left[\frac{kJ}{m^2 s}\right]$
Methane	1260
Methanol	919413
Ethanol	1170497
Gas	1553790
LPG	4005

5.2. Order of reaction and combustion rate

The burning velocity refers to the rate at which fuel undergoes combustion. It is defined as the linear regression of the fuel in parallel layers perpendicular to the surface itself. It can also be described as the distance traveled by the flame front into the fuel over a unit of time under known pressure and temperature conditions. Factors influencing the burning rate include pressure, the initial temperature of the fuel, fuel composition, and the size of oxidizer particles. The laminar burning velocity, or the speed at which the flame propagates, is given by the following formula:

$$u_L = \lim_{t \to 0} \frac{\Delta x}{\Delta t} = \frac{dx}{dt} \quad (29)$$

where: $\frac{dx}{dt}$ – the rate of the combustion reaction depends on the order of the reaction.

Table 8. The combustion rate of individual fuels [1]

Fuel	Combustion speed $\left[\frac{m}{s}\right]$
Methane	0.38–0.45
Methanol	0.2–0.3
Ethanol	0.3–0.35
Gas	0.3–0.45
LPG	0.35–0.4

The burning velocities of individual fuels can vary within specific ranges. For each fuel, the possible range of velocities achievable under different conditions is presented. Factors such as the fuel-to-oxidizer ratio, initial temperature, and pressure influence the burning velocity [9].

The order of a reaction determines how the rate of a chemical reaction depends on the concentrations of its reactants. First-order reactions involve the transformation of a single molecule. Second-order reactions involve the formation of products through the interaction of two molecules. Third-order reactions involve the simultaneous interaction of three atoms or molecules, making such reactions relatively rare.

The differential equations for first- and second-order reactions are as follows:

$$\frac{dx}{dt} = k_1(a - x) \tag{30}$$

$$\frac{dx}{dt} = k_2(a - x)^2 \tag{31}$$

or

$$\frac{dx}{dt} = k_2(a - x)(b - x) \tag{32}$$

where: a/b – initial concentration of substance A/B, x – the amount of substance A/B undergoing transformation during time t, k_1/k_2 – reaction rate constant for 1st and 2nd order reactions.

Combustion can be treated as a first- or second-order reaction, depending on the conditions. During combustion with an excess of oxygen, it is assumed that the oxygen concentration remains practically constant throughout the reaction. In such cases, the reaction rate will primarily depend on the concentration of the combustible substance.

Methane

$$\frac{dx}{dt} = k_1\left(a_{CH_4} - x_{CH_4}\right) \tag{33}$$

Methanol

$$\frac{dx}{dt} = k_1\left(a_{CH_3OH} - x_{CH_3OH}\right) \tag{34}$$

Ethanol

$$\frac{dx}{dt} = k_1\left(a_{C_2H_5OH} - x_{C_2H_5OH}\right) \tag{35}$$

Gas

$$\frac{dx}{dt} = k_1\left(a_{C_8H_{18}} - x_{C_8H_{18}}\right) \tag{36}$$

LPG

During the combustion of a mixture of two gases, the reaction rate is considered separately for each of them.

$$\frac{dx}{dt} = k_1\left(a_{C_3H_8} - x_{C_3H_8}\right) \tag{37}$$

$$\frac{dx}{dt} = k_1\left(a_{C_4H_{10}} - x_{C_4H_{10}}\right) \tag{38}$$

The key to understanding the kinetics of combustion reactions lies in the reaction order and burning velocity. These parameters enable the prediction of combustion rates for various fuels under identical or varying conditions. This understanding is critical in the fields of chemical engineering, energy production, and environmental protection. Knowledge of reaction kinetics also allows for the optimization of combustion processes, minimizing the emission of harmful substances while maximizing efficiency.

5.3. Fuel consumption

To determine the fuel requirements, an analysis of the fuel-air mixture mass was conducted for various types of fuels. It was assumed that the mass of fuel injected in a single cycle is 50 mg. The calculations accounted for the theoretical air demand relative to the fuel mass. The fundamental relationship describing the mass of the fuel-air mixture is expressed by the formula:

$$m_{mix} = m_{fuel} + m_{air} \tag{39}$$

where: m_{fuel} – mass of fuel [mg], m_{air} – air mass required for the combustion of a given amount of fuel [mg].
The air mass has been determined by the formula:

$$m_{air} = L_t \cdot m_{fuel} \tag{40}$$

The mixture mass calculations for methane have been performed:

$$m_{mix} = 50\ \text{mg} + 17.2 \cdot 50\ \text{mg} \tag{41}$$

$$m_{mix} = 910\ \text{mg}$$

Analogous calculations were performed for each fuel, and the results are presented in the table below.

Table 10. Calculation results for the individual mixture masses for one cycle

Fuel	Mass of mixture [mg]
Methane	910
Methanol	370
Ethanol	500
Gas	785
LPG	830

6. Numerical analysis of a sample engine

6.1. Simulation environment and boundary parameters

ANSYS Fluent software was utilized to model the processes occurring in the pulse jet engine. The analysis was conducted on a valved pulse jet engine model with a combustion chamber designed in accordance with the calculations from Chapter 5. The process began with the preparation of a two-dimensional geometry in ANSYS Discovery, followed by generating a computational mesh using ANSYS Fluent's built-in mesh generator. The element size was set to 10^{-3} m, providing relatively high mesh density in critical areas for accurate representation of flow phenomena and exhaust gas generation. The standard Fluent mesh type and default settings, such as growth rate and mesh quality control methods (smoothing and remeshing), were used without modifications.

The resulting computational mesh was denser in the fuel injection zone, enabling a more detailed analysis of the mixing processes between fuel and air and the formation of the reaction zone. This area exhibited locally higher node density, minimizing numerical errors associated with the rapid changes in the physicochemical properties of the flow. A sample view of the mesh in the fuel injection region is shown in Fig. 4, where the increased mesh density in the diffusion zone of the fuel is clearly visible.

The next step was to define an appropriate turbulence model. The k-omega Shear Stress Transport (SST) model, a second-order accuracy model, was chosen. This model was selected due to its high efficiency in describing flows with strong velocity and pressure gradients, which are particularly relevant in cases involving intense fuel-air mixing and wall-bounded phenomena in flow channel regions. The k-omega SST model combines the advantages of the k-epsilon model in free-stream regions with the characteristics of the k-omega model in near-wall zones, providing a more accurate analysis of the phenomena.

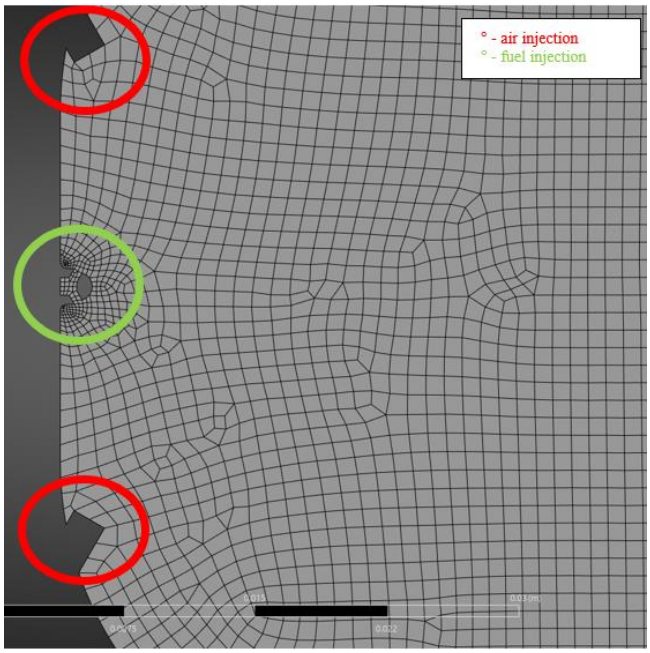

Fig. 4. Mesh of the fuel and air injection and mixing area

For modeling the combustion process, the Non-Premixed Combustion method was implemented, enabling the representation of chemical reactions in systems with separate fuel and oxidizer supplies. This type of model is often applied in systems where fuel and air mix within the flow zone (e.g., fuel injection in the intake duct or combustion chamber). Non-Premixed Combustion uses the concepts of the mixture field and mixture fraction, allowing for the consideration of diverse local conditions in terms of temperature, chemical composition, and enthalpy.

To ensure computational stability and achieve satisfactory convergence, standard second-order upwind schemes were applied for transport equations and the energy equation. This choice was dictated by the need to accurately capture rapid temperature and velocity gradient changes, particularly in the combustion reaction zone. The iterative process was conducted until the residual error values dropped below the accepted 2% threshold, indicating the stabilization of key flow and thermodynamic parameters within the computational domain [2, 29].

6.2. Simulation study results

To investigate the flow dynamics and fuel combustion processes within the chamber, a simulation was conducted for a single injection under static (steady-state) conditions. This assumption enabled the analysis of key parameters crucial for design optimization: velocity distribution, heat release rate, and dynamic pressure. The importance of these parameters lies in the need to select an appropriate chamber geometry and determine an effective method for fuel-air mixing, which ultimately influences combustion efficiency and engine stability.

Each combustion simulation assumed a fuel injection of 50 mg and a corresponding air dose, calculated based on stoichiometric conditions specific to the analyzed fuel. This standardized approach ensured comparable initial conditions across all studied variants and allowed for the assessment of individual parameters' impacts on combustion efficiency.

The results obtained highlight the need for design modifications aimed at optimizing the shape of the combustion chamber and adjusting the fuel injection and air supply systems to diverse operating conditions. Notably, a strong correlation was observed between the distribution of velocity and dynamic pressure fields and parameters related to combustion reaction kinetics. Uniform distribution of the mixture within the chamber is a key factor in minimizing heat losses and thereby ensuring high efficiency of the propulsion system.

The subsequent sections present detailed simulation results, including:

– Velocity gradients – allowing the identification of areas with high and low local flow values
– Heat release rate – enabling the determination of combustion process intensity
– Dynamic pressure – crucial for assessing the structural strength of components and potential wave phenomena in the chamber.

The analysis of these parameters provides insights for further engine optimization in terms of operational stability, thermodynamic performance, and adaptability to different types of fuels.

In the case of methane combustion (Fig. 5–7), a relatively uniform velocity field is observed in the central part of the stream, indicating stable mixing of fuel with air. The heat release gradient (Fig. 6) is primarily concentrated in the region immediately downstream of the injection point, where the main oxidation process of methane begins.

Methane

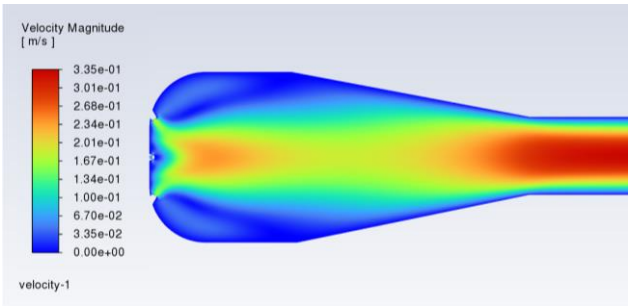

Fig. 5. Velocity gradient for methane combustion

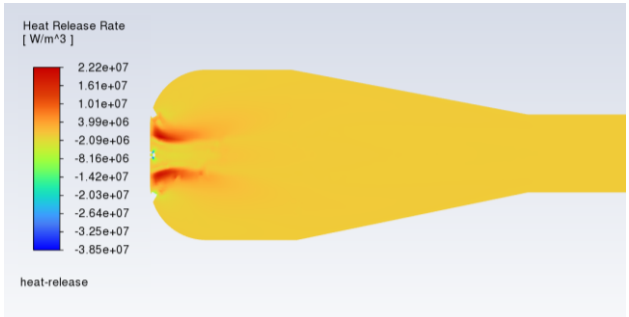

Fig. 6. Heat release gradient for methane combustion

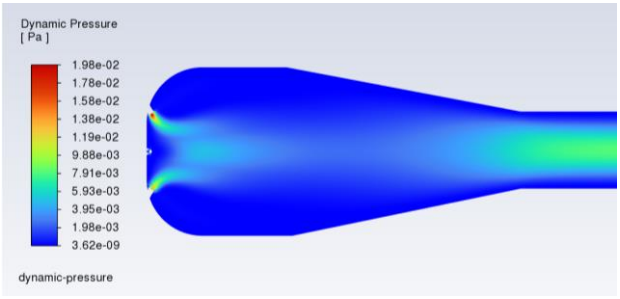

Fig. 7. Dynamic pressure gradient for methane combustion

Meanwhile, the dynamic pressure distribution (Fig. 7) suggests that pressure values stabilize further along the stream, which may indicate a relatively smooth progression of the combustion process. These results confirm that methane exhibits favorable combustion conditions under the simulated conditions.

Methanol

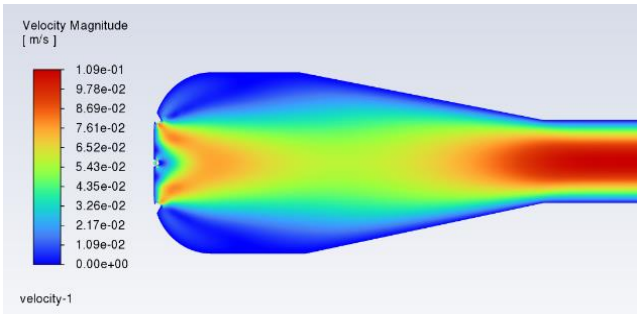

Fig. 8. Velocity gradient for methanol combustion

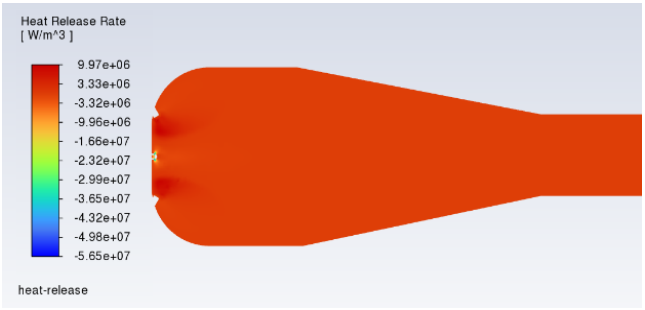

Fig. 9. Heat release gradient for methanol combustion

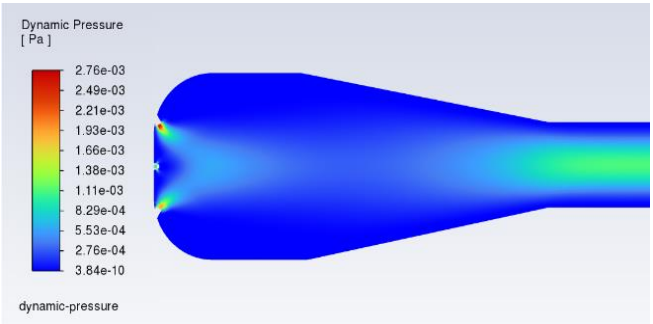

Fig. 10. Dynamic pressure gradient for methanol combustion

The results presented in Fig. 8–10 show that, for methanol combustion, the maximum velocity values (Fig. 8) occur in the central part of the stream, with a relatively narrow combustion zone located near the injection point. The heat release rate (Fig. 9) is notably intense during the initial phase of combustion, resulting in a more pronounced temperature gradient. The dynamic pressure distribution (Fig. 10) is similar to that of methane, although slightly higher values are observed locally in the reaction zone. This may indicate a faster oxidation process for methanol, attributed to its favorable physicochemical properties, such as a lower ignition temperature and the ease of forming a combustible mixture with air.

Ethanol

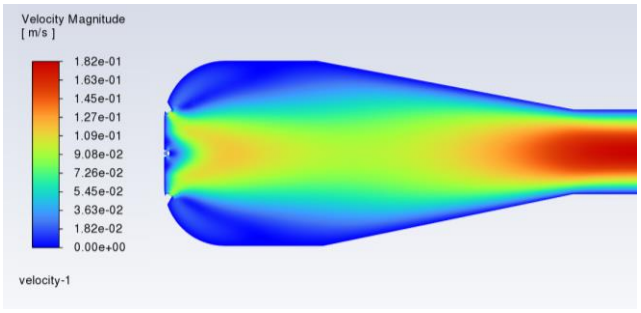

Fig. 11. Velocity gradient for ethanol combustion

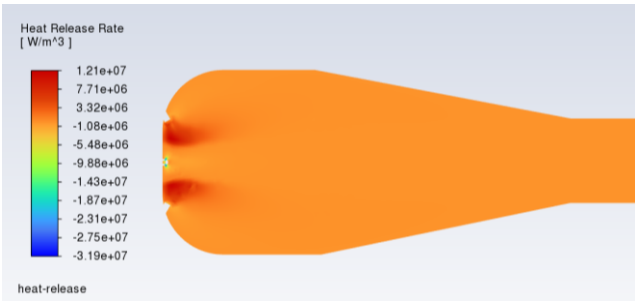

Fig. 12. Heat release gradient for ethanol combustion

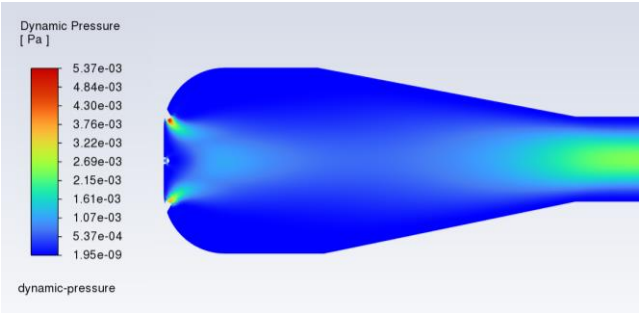

Fig. 13. Dynamic pressure gradient for ethanol combustion

In the case of ethanol (Fig. 11–13), the velocity distribution (Fig. 11) is relatively uniform, with the zone of highest velocity values extending along the axis of the stream. The heat release intensity (Fig. 12) is slightly lower in the initial combustion zone compared to methanol, which may indicate a milder nature of the preliminary reaction. Meanwhile, the dynamic pressure (Fig. 13) shows a noticeable increase in the combustion zone but returns to lower values further downstream. This behavior may result from the uniform propagation of the flame front and the relatively

high energy content of ethanol, coupled with its moderate boiling temperature, which facilitates efficient evaporation within the chamber.

Gas

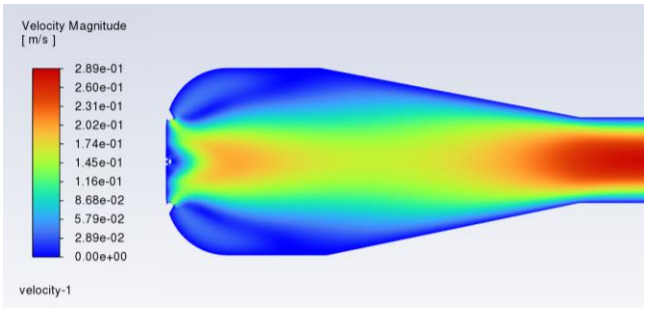

Fig. 14. Velocity gradient for gasoline combustion

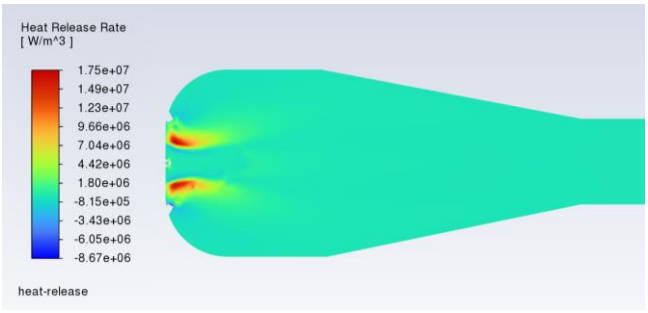

Fig. 15. Heat release gradient for gasoline combustion

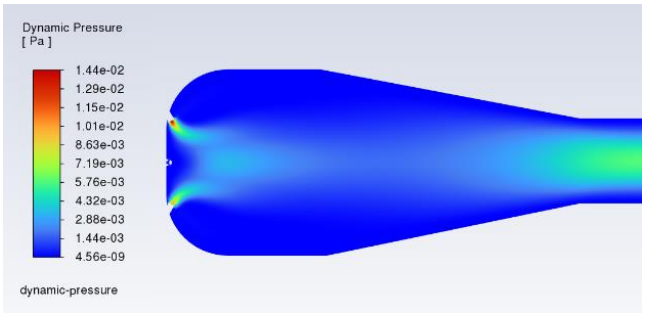

Fig. 16. Dynamic pressure gradient for gasoline combustion

For gasoline combustion (Fig. 14–16), the widest distribution of the high-velocity zone is observed (Fig. 14), which may result from the more complex chemical structure of the fuel and the higher volatility of hydrocarbon fractions. The heat release gradient (Fig. 15) suggests a multi-stage combustion process, with visible points of intense energy release near the injection point and in adjacent regions, indicating possible variations in reactions depending on local mixing conditions. The dynamic pressure distribution (Fig. 16) is significantly higher near the injection point, followed by a gradual decrease further along the stream. This indicates potential challenges in achieving uniform distribution of the fuel-air mixture, which may necessitate additional modifications to the chamber design.

LPG

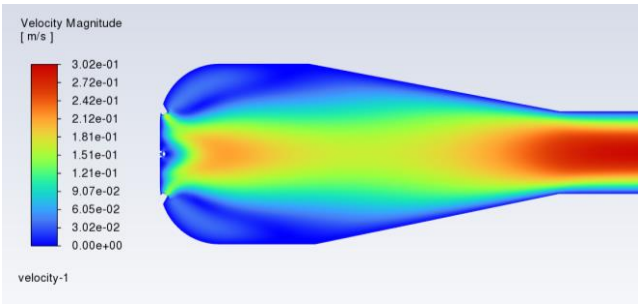

Fig. 17. Velocity gradient for LPG combustion

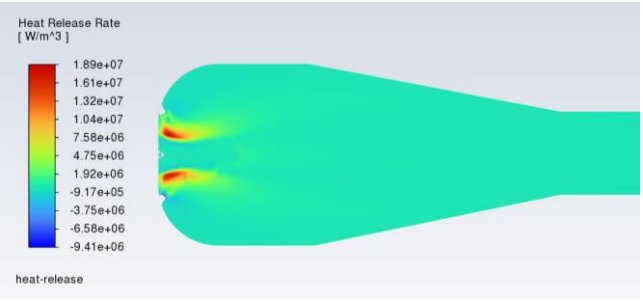

Fig. 18. Heat release gradient for LPG combustion

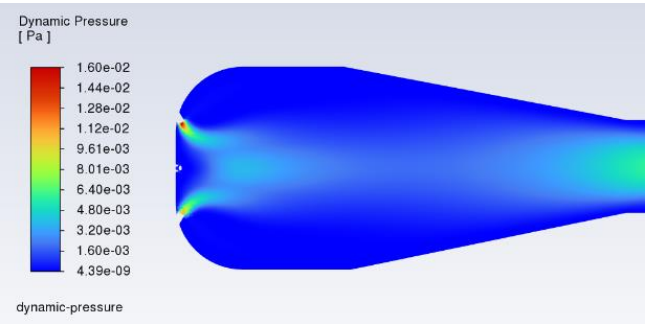

Fig. 19. Dynamic pressure gradient for LPG combustion

Simulations for LPG combustion (Fig. 17–19) confirm high flow velocity (Fig. 17) in the central zone, with a distinct concentration of the combustion process near the injection point. The thermal distribution (Fig. 18) indicates a high level of heat release within a small area, which may pose challenges related to heat dissipation and flame stability. The dynamic pressure (Fig. 19) shows relatively high values in the initial region, which diminish as the combustion progresses toward the outlet. From the perspective of integration into a multi-fuel system, LPG could prove advantageous due to its rapid evaporation and mixing capabilities with air. However, careful chamber design is required to address its relatively high thermal potential and dynamic pressure near the injection point.

7. Design solutions

Adapting a pulse jet engine to operate on methane, methanol, ethanol, gasoline, and liquefied petroleum gas (LPG) necessitates comprehensive modifications to accommodate the distinct thermophysical and chemical properties of each fuel.

A universal injection system must be designed to manage considerable variations in viscosity, density, and evaporation temperature. This includes the judicious selection of nozzle dimensions and injection pressures to achieve effective atomization and uniform mixing with the air stream. Additionally, a flexible ignition system – capable of modulating spark energy or ignition timing – must account for disparate ignition temperatures and heat of vaporization, while enhanced thermal and corrosion-resistant materials are required to protect critical regions of the combustion chamber from degradation [10].

The air intake and exhaust assemblies must also incorporate mechanisms for precise flow regulation, such as valves or variable airflow control elements, in order to maintain optimal stoichiometric ratios for each fuel. These modifications help to prevent local thermal hotspots and incomplete combustion. Moreover, improvements to the cooling configuration may be warranted to ensure sufficient heat dissipation and avert structural damage in high-temperature zones.

Implementing a real-time monitoring and control system – integrating temperature, pressure, and exhaust gas composition sensors – is imperative for dynamically adjusting engine parameters. This feedback loop enables consistent and safe operation across a variety of fuels by continuously optimizing combustion conditions and detecting anomalous performance indicators.

Finally, an integrated fuel and air injection methodology (Fig. 20) initiates the mixing process directly at the injector outlet, thus reducing the overall number of components and enhancing mixture homogeneity.

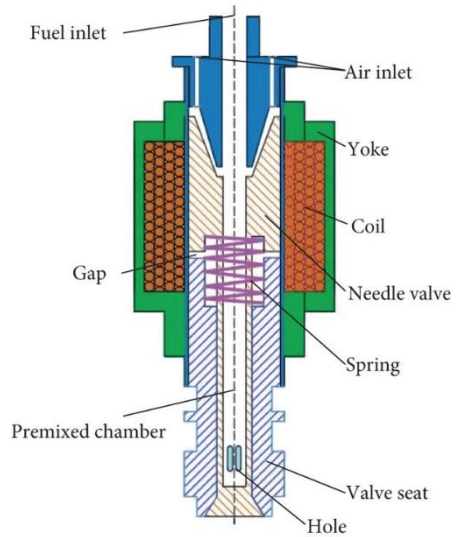

Fig. 20. Example of a fuel-air injector [6]

This approach further streamlines engine control and promotes stable combustion, facilitating a robust and efficient multi-fuel pulse jet engine design.

A promising approach involves implementing a variable-position fuel injector, wherein the injector's angular orientation with respect to the combustion chamber is dynamically adjusted to optimize the spatial distribution and mixing of the fuel–air mixture. This adaptability also accommodates variations in fuel properties (e.g., viscosity, volatility, and density) that influence diffusion dynamics within the chamber (Fig. 21).

Fig. 21. Example of a flexible joint adapter for a fuel injector [28]

Another critical design consideration concerns the geometry of the combustion chamber. The velocity gradient (Fig. 22) reveals that flow regions outside the primary combustion zone incur superfluous losses and reduce overall engine efficiency. While increasing the injection dose offers one potential remedy, this approach is not fully scalable and may introduce instability into engine operation.

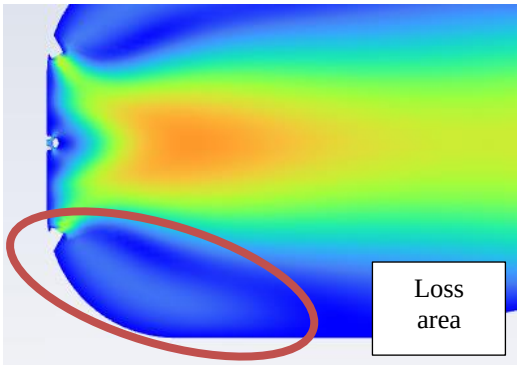

Fig. 22. Example of an area with suboptimal flow

A further design consideration involves implementing variable geometry for the exhaust channel, a feature closely tied to the formation of standing waves that are crucial for achieving stable and efficient engine operation. By enabling adjustments to the channel length, one can precisely tune the standing wave position, thereby ensuring consistent performance.

8. Conclusions

The viability and potential of a multi-fuel pulse jet engine capable of operating on various fuels – including methane, methanol, ethanol, gasoline, and LPG – has been demonstrated both theoretically and numerically. Addressing modern military requirements and advancing research into valved pulsejet propulsion necessitates this versatile approach to fuel selection, as the ability to adapt to different energy sources is of paramount strategic importance. From a scientific perspective, developing such flexibility broadens opportunities for future experimental and defense-related applications.

The use of numerical simulations in the ANSYS Fluent environment enabled a detailed analysis of key engine performance parameters, such as velocity distribution, dynam-

ic pressure, and heat release rate. Based on these results, it was concluded that effective mixing of fuel and air in the combustion chamber is a critical condition for achieving a stable and efficient combustion process. Simultaneously, the findings highlight the need for several design modifications, including considerations of the varied calorific values, viscosity, air demand, evaporation temperature, and different cooling and material resistance requirements of the fuels.

The obtained results demonstrate the high potential of the multi-fuel pulse jet engine concept for both experimental and military applications. At the same time, they emphasize the need for further research, including experimental validation of the simulation results and continued improvements to the design. The successful implementation of a multi-fuel pulse jet engine will require interdisciplinary development efforts in fluid mechanics, thermodynamics, materials science, and control systems, presenting broad opportunities for the advancement of this technology.

Acknowledgements

This work was supported by the Research Subsidy SBAD: 0416/SBAD/0007 in the year 2025.

We would like to express our sincere thanks to the members of the PUT JET Riders scientific group for their help during the research.

Nomenclature

CFD	computational fluid dynamics
CFX	a software used for computational fluid dynamics
H_{mx}	maximum energy during combustion
LPG	liquefied petroleum gas
SST	Shear Stress Transport model
ΔH°	enthalpy of reaction

Bibliography

[1] Atkins PW. Chemia fizyczna III. Wydawnictwo Naukowe PWN. Warszawa 2022.

[2] Bajerlein M, Karpiuk W, Smolec R. Application of gas dissolved in fuel in the aspect of a hypocycloidal pump design. Energies. 2022;15:9163. https://doi.org/10.3390/en15239163

[3] Bradley D, Cheng RK, Dunn-Rankin D, Evans RL, Keller J, Levinsky H et al. Lean combustion. Dunn-Rankin D (ed.) Academic Press 2008.

[4] Candel S, Durox D, Ducruix S, Birbaud AL, Noiray N, Schuller T. Flame dynamics and combustion noise: progress and challenges. Int J Aeroacoust. 2009;8(1): 1-56. https://doi.org/10.1260/147547209786234984

[5] Czarnigowski J, Skiba K, Dubieński K. Investigations of the temperature distribution in the exhaust system of an aircraft piston engine. Combustion Engines. 2019;177(2):12-18. https://doi.org/10.19206/CE-2019-203

[6] Du B, Zhao Z. Experimental investigation on the effects of injection parameters on the air-assisted diesel spray characteristics. Int J Aerospace Eng. 2022;2022: 1-21. https://doi.org/10.1155/2022/6814732

[7] Garnier E, Leplat M, Monnier JC, Delva J. Flow control by pulsed jet in a highly bended s-duct. 6th AIAA Flow Control Conference 2012;2012-3250. https://doi.org/10.2514/6.2012-3250

[8] Ghulam MM, Muralidharan SS, Anand V, Prisell E, Gutmark EJ. Operational mechanism of valved-pulsejet engines. Aerosp Sci Technol. 2024;148: 109060. https://doi.org/10.1016/j.ast.2024.109060

[9] Haynes WM, Lide DR, Bruno TJ. CRC handbook of chemistry and physics. 95th ed. 2014.

[10] Idzior M, Karpiuk W, Smolec R. Investigation of novel ceramic materials (Al_2O_3 and SSiC) for high-pressure pumps delivery sections. Combustion Engines. 2024;196(1):153-160. https://doi.org/10.19206/CE-174315

[11] Johnson RG. Design, characterization, and performance of a valveless pulse detonation engine. Monterey. Thesis and Dissertation. 2000. http://ndl.handle.net/10945/7664

[12] Kozak M, Merkisz J. Oxygenated diesel fuels and their effect on PM emissions. Appl Sci. 2022;12(15): 7709. https://doi.org/10.3390/app12157709

[13] Lijewski P, Kozak M, Fuć P, Rymaniak Ł, Ziółkowski A. Exhaust emissions generated under actual operating conditions from a hybrid vehicle and an electric one fitted with a range extender. Transp Res D Transp Environ. 2020;78:102183. https://doi.org/10.1016/j.trd.2019.11.012

[14] Meyer R, Köhler J, Homburg A. Explosives. Wiley 2007:422. https://onlinelibrary.wiley.com/doi/book/10.1002/9783527617043

[15] Min L, Ling Y, Wen-xiang C. Experiment analysis of combustion performance in pulse jet engine. Enrgy Proced. 2016:248-252. https://doi.org/10.1016/j.egypro.2016.10.173

[16] Moran MJ, Shapiro HN. Fundamentals of engineering thermodynamics. Wiley 2008.

[17] National Institute of Standards and Technology. NIST Chemistry WebBook. https://webbook.nist.gov/chemistry/form-ser/ (accessed on 2025.01.04).

[18] National Institute of Standards and Technology. NIST Chemistry WebBook. https://webbook.nist.gov/chemistry/rea (accessed on 2025.01.05).

[19] Pielecha I. Numerical investigation of lambda-value prechamber ignition in heavy duty natural gas engine. Combustion Engines. 2020;181(2):31-39. https://doi.org/10.19206/CE-2020-205

[20] RAND Corporation. Pulsejet engines for UAVs: flight-proven drone propulsion systems. 2012.

[21] Sawan Kumar G. Experimental studies on a valveless pulsejet engine. https://www.researchgate.net/publication/366759940
[22] Serridge M, Licht TR. Piezoelectric accelerometers and vibration preamplifiers. Brüel & Kjær 1987.
[23] Warimani M, Azami MH, Ismail AF. Study of feasibility of pulse detonation engine powered by alternative fuels 292. Int J Eng Adv Technol. 2019;8(2S2): 291-296. www.ijeat.org
[24] Wikipedia. Pulsjet cross-section. https://en.wikipedia.org/wiki/Pulsejet#/media/File:Puls1Motor_en.gif
[25] Wikipedia. Pulsejet work cycle image. https://en.wikipedia.org/wiki/Pulsejet#/media/File:Pulse_Jet_Engine.PNG
[26] Wójcicki S. Silniki pulsacyjne strumieniowe i rakietowe. Wydawnictwo Ministerstwa Obrony Narodowej. Warszawa 1962.
[27] Wójcicki S. Spalanie. Wydawnictwa Naukowo-Techniczne. Warszawa 1969.
[28] Zakład urządzeń pomiarowych (in Polish). https://www.zup.com.pl/index.php/katalog/adapter-przegubowy-do-wyciagacznia-wtryskiwaczy.html (accessed on 2025.03.04).
[29] Zhou L, Wang W. LES of propane-air swirling non-premixed flame using a SOM combustion model. Combustion Engines. 2025;200(1):71-77. https://doi.org/10.19206/CE-197157

Prof. Grzegorz M. Szymański, DSc., DEng. – Institute of Transport, Poznan University of Technology, Poland.
e-mail: *grzegorz.m.szymanski@put.poznan.pl*

Klaudia Strugarek, Eng. – Institute of Transport, Poznan University of Technology, Poland.
e-mail: *klaudia.strugarek@student.put.poznan.pl*

Malwina Nowak, Eng. – Institute of Chemical Technology and Engineering, Poznan University of Technology, Poland.
e-mail: *malwina.nowak@student.put.poznan.pl*

Aleksander Ludwiczak, Eng. – Institute of Transport, Poznan University of Technology, Poland.
e-mail: *aleksander.ludwiczak@student.put.poznan.pl*

Prof. Bogdan Wyrwas, DSc., DEng. – Institute of Technical Chemistry and Electrochemistry, Poznan University of Technology, Poland.
e-mail: *bogdan.wyrwas@put.poznan.pl*

Alicja Szymańska, – Institute of Technical Chemistry and Electrochemistry, Poznan University of Technology, Poland.
e-mail: *alicja.szymanska.1@student.put.poznan.pl*

Mikołaj Klekowicki, Eng. – Institute of Transport, Poznan University of Technology, Poland.
e-mail: *mikolaj.klekowicki@student.put.poznan.pl*